

## EFFECT OF PAVEMENT SURFACE TEXTURE ON BRITISH PENDULUM TEST

Yang Pin Kelvin LEE  
Pavement Engineer  
Samwoh Asphalt Premix Pte Ltd  
25E Sungei Kadut Street 1  
Singapore 729333  
E-mail: kelvinlee@samwoh.com.sg

Tien Fang FWA  
Professor  
Center for Transportation Research  
Dept of Civil Engineering  
National University of Singapore  
10 Kent Ridge Crescent  
Singapore 119260  
Fax: 65-6779-1635  
E-mail: cvefwatf@nus.edu.sg

Yoo Sang CHOO  
Associate Professor  
Dept of Civil Engineering  
National University of Singapore  
10 Kent Ridge Crescent  
Singapore 119260  
E-mail: cvecys@nus.edu.sg

**Abstract:** The British pendulum tester is commonly used for the measurement of skid resistance of pavement surfaces. Although it is widely suggested that the measurement is largely governed by the microtexture of the pavement surface, experience has shown that the macrotexture can also affect the measurements. It can also lead to misleading results on coarse-textured test surfaces. This paper reports the findings of a study conducted to examine the effect of macrotexture on the British pendulum measurements. The study employed a three-dimensional finite element model to analyze the behavior of the test device. The results of the analysis showed significant variations of test results on sparsely spaced textured surfaces, especially those that exhibited discontinuities. The results demonstrated that the edge impacts between coarse-textured surface features and the pendulum slider would give rise to unreliable test measurements.

**Key Words:** British pendulum tester, finite element model, pavement surface texture, skid resistance

### 1. INTRODUCTION

The British pendulum tester (Giles et al., 1964) is one of the simplest and cheapest instruments used in the measurement of friction characteristics of pavement surfaces. It is extremely versatile in its applications to many test situations and has received acceptance worldwide. The test device measures low-speed friction (about 10 km/h) and is commonly used to assess the microtexture of pavement surfaces.

However, studies by Fwa et al. (2003) and Liu et al. (2004) have shown that the British pendulum measurements can be affected by the macrotexture of pavement surfaces. Moreover, past studies (Forde et al, 1976, Salt, 1977, Purushothaman et al., 1988) also reported that the British pendulum tester exhibited unreliable behavior when tested on coarse-textured surfaces.

The objective of this study is to examine the effect of macrotexture on the British pendulum test measurement and to provide a better understanding of the behavior of the test device on coarse-textured surfaces such as grooved and porous surface pavements. The study comprises laboratory test and finite element simulation. The ability of finite element modeling to simulate the British pendulum test has already been demonstrated by Liu et al. (2003) and Lee et al. (2004). The models were shown to provide a valid representation of the British pendulum test and offer a useful tool to analyze the test behavior of the device. Besides providing a means to assess the frictional resistance of pavement materials without the need to fabricate the test specimens, the finite element solutions offer other information such as contact stresses which cannot be easily obtained experimentally.

## **2. LABORATORY TEST ON EFFECT OF MACROTEXTURE**

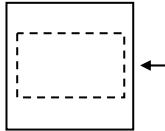
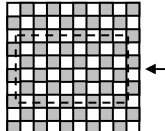
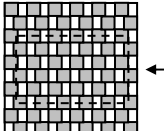
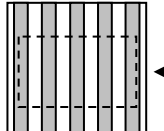
The test program was designed to study the effect of macrotexture on the British pendulum measurement. The evaluation was conducted with respect to two macrotexture parameters, namely, aggregate size and aggregate gap width or spacing between aggregates. These parameters were shown to have direct effects on the British pendulum measurements according to Fwa et al. (2003) and Liu et al. (2004). The test specimens were fabricated using Portland cement mortar and the test surface were made up of idealized aggregate patterns with textural features of different sizes, spacing and shapes.

### **2.1 Specimen Preparation**

A mortar mix of cement-to-sand ratio of 1:2 and cement-to-water ratio of 1:0.4 was used to cast the specimens. The surface dimensions of the specimens were 150 mm by 150 mm and 60 mm thick. These dimensions were selected in accordance to ASTM E303-93 (ASTM, 2000) to accommodate for a sliding distance of about 127 mm for the British pendulum test.

Three types of textured surfaces were considered as shown in Table 1. Set A consisted of square aggregates with variable sizes and gap widths ranging from 5 mm to 25 mm. Set B consisted of single-size square aggregates (15 mm x 15 mm) with variable gap widths. Set C consisted of rectangular strips with variable groove width. The height of the exposed aggregates or the depth of the grooves was fixed at 5 mm. In addition, a plain surface texture was introduced to serve as a reference for comparison. Three replicates were cast for each type of specimen.

Table 1. Description of texture patterns for laboratory test

Set	Reference	A	B	C
Plan View				
Details	Plain Surface	Square aggregates with variable size and spacing from 5mm to 25mm	15mm square aggregates with variable gap width from 5mm to 15mm in direction of sliding	15mm wide rectangular strips with variable groove width from 5mm to 15mm in direction of sliding

Note: 1) Arrow denotes sliding direction. 2) Broken-line rectangle indicates sliding path.

## 2.2 Analysis of Laboratory Test Results

The tests were conducted under dry and wet test conditions and the results are reported as the average British pendulum number (BPN) as shown in Figure 1. The results showed that the BPN decreases as aggregate gap width increases for dry and wet case respectively. This agreed well with the findings of Fwa et al. (2003) and Liu et al. (2004) which revealed that the decreasing trend of the BPN was largely attributed to the decrease in contact area as well as number of aggregate gaps within the sliding area as gap width increases. The former contributes to the adhesion component of friction while the latter contributes to rubber deformation. These are two important mechanisms which contribute to rubber friction (Moore, 1972). In comparison with the results obtained on a plain surface, it is noted that the increase in BPN of the textured surfaces of Set C specimens over those of plain surfaces were about two times larger than those of Set A and B specimens.

The BPN results for the various test specimens were also plotted with respect to contact area and number of gap widths as shown in Figure 2. For Set A specimens, the increasing BPN at constant contact area were attributed to the increasing number of gaps as gap width decreases. In the case of Set B and C specimens, both the contact area and number of gaps contributed to the increasing BPN as aggregate gap reduces. However, it is interesting to note that Set C specimens exhibited significantly larger BPN as compared to those of Set A and B specimens even for cases where the contact area or number of gaps are lesser than those of Set A and B. As such, it is likely that there other factors which can affect the BPN. In order to provide in-depth analysis on the test results, finite element modeling is used to investigate the phenomenon. This is described in the next section.

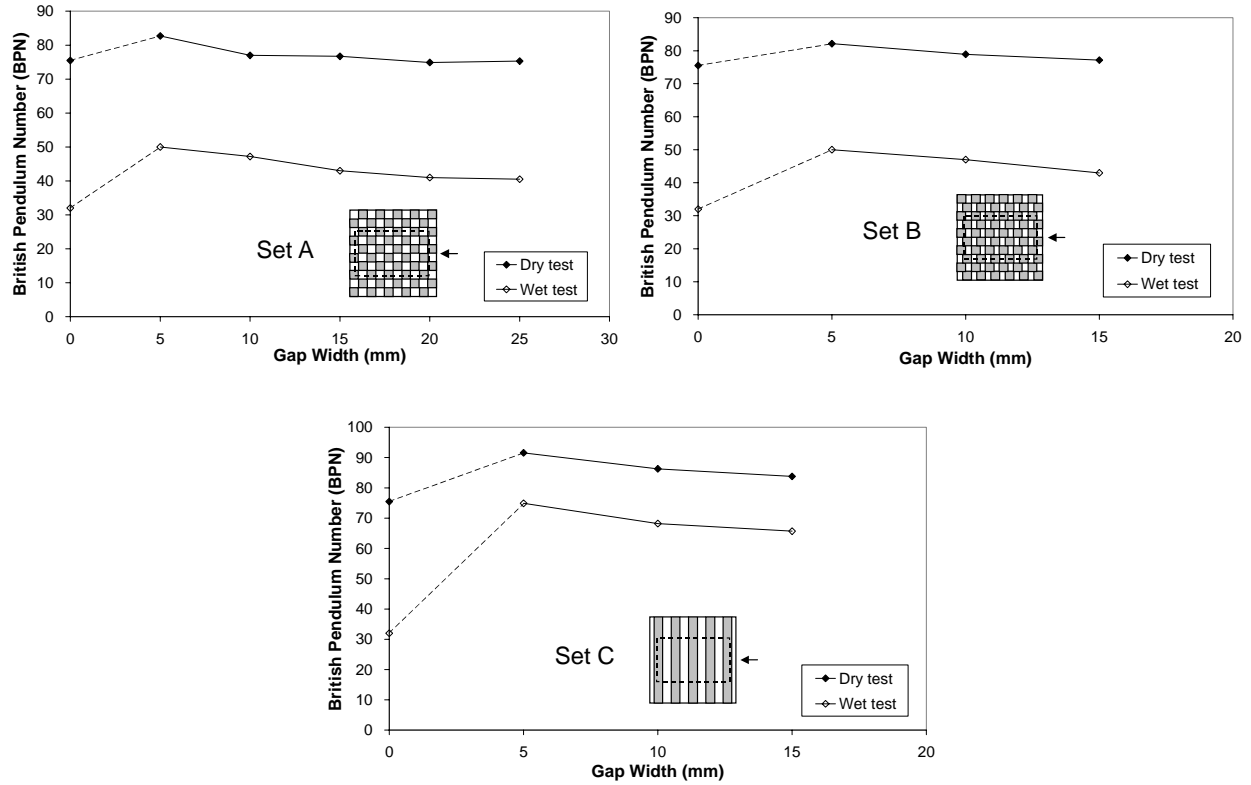


Figure 1. Laboratory British pendulum measurements

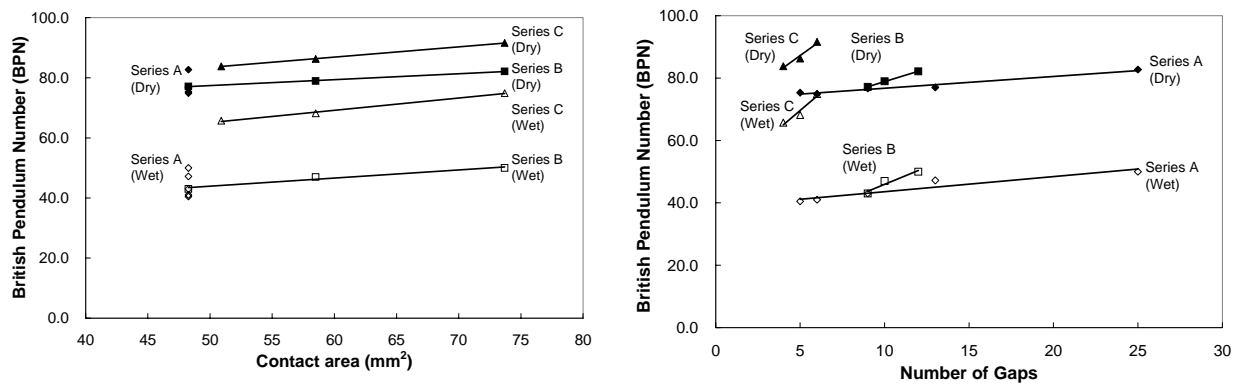


Figure 2. Effect on contact area and aggregate gaps on the British pendulum measurements

### 3. FINITE ELEMENT MODELING

The finite element model developed by Lee et al. (2004) was used in this study. The analysis was conducted using the finite element software, ABAQUS/Explicit (Hibbitt, Karlsson & Sorensen Inc., 2002). The key features of the finite element model are described in the following sub-sections.

### 3.1 Geometric Representation

The loading mechanism of the finite element model was represented based on the actual mechanism of the British pendulum tester as shown in Figure 3. A spring housed under tension within the pendulum arm is connected to a lever system to transmit a downward force on the test surface. Sliding at the contact point between the pivot arm and the lever system was permissible to provide allowance for the rubber slider to move vertically up and down when it slides along the test surface. The sliding interaction was modeled using a sliding contact constraint (SLIDER) available in ABAQUS. The driving force for the test is the mass of the pendulum, which is 1.486 kg with a center of gravity at a distance of 410 mm from the pivot as specified according to ASTM (2000). The densities of the various components of the pendulum model were defined according to laboratory measurements.

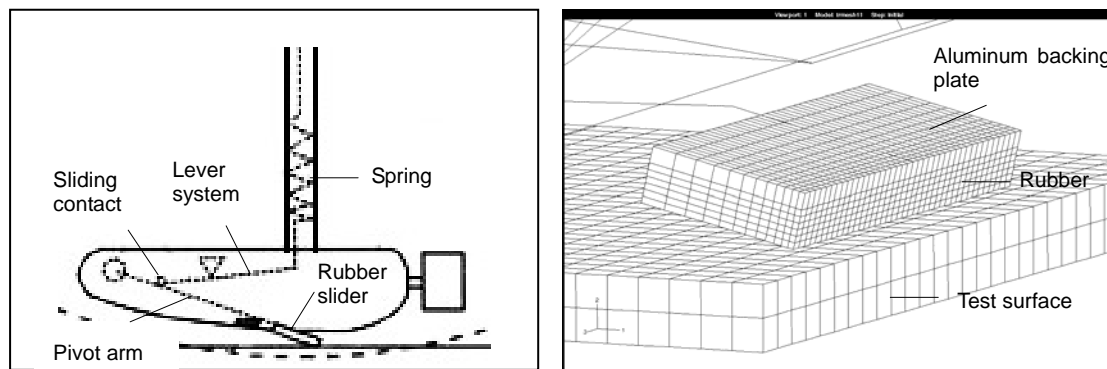


Figure 3. *Left:* Loading mechanism of the British pendulum tester; *Right:* 3D view of finite element mesh at rubber-pavement interface

### 3.2 Element Types and Material Properties

The rubber, aluminum backing plate and test specimen were defined using hexahedral elements (shown in Figure 3) and the spring was defined using a connector element (SPRINGA). The pendulum arm, pivot arm and lever system were defined using beam and truss elements. The stiffness of the spring was determined by comparing the normal force acting on the test surface between the simulation results and experimental measurements. Being much stiffer as compared to the rubber, typical values for the elastic modulus of aluminum of  $72.4 \times 10^3$  MPa and Poisson's ratio of 0.33 (Higdon and Ohlsen, 1971) were defined for the aluminum backing plate, pendulum arm, pivot arm and lever system as they would not have any significant implication on the displacement or deformation of the spring and rubber. Similarly for the test specimen, typical values for the elastic modulus of Portland cement mortar of  $27.6 \times 10^3$  MPa and Poisson's ratio of 0.15 (Huang, 1993) were adopted. The rubber was modeled as a hyperelastic material using the Arruda-Boyce strain energy function (Arruda and Boyce, 1993), which was found to be an appropriate model to describe the behavior of the rubber slider. The material constants were derived from regression analysis based on experimental test data obtained from uniaxial compression test.

### 3.3 Prescribed Conditions and Constraints

To reduce computational time, the finite element analysis started at the instant when the rubber slider made its first contact with the test surface. An initial velocity of about 2.8 m/s (computed based on conservation of energy) was applied at all nodes in the pendulum model. A hinge was imposed at the top of the pendulum arm to allow for rotation of the pendulum and the bottom surface of the pavement was fixed to prevent any displacement.

### 3.4 Contact and Interaction Modeling

The sliding between the rubber slider and test specimen was simulated using the surface-based contact mode available in ABAQUS. The contact boundaries between the slider and test specimen were represented by two deformable surfaces. The contact constraint was enforced using a penalty algorithm. A master and slave surface contact pair was defined where the elements of the rubber were defined as the slave surface while those of the test surface were defined as the master surface. The classical Coulomb friction model was defined at the contact surface and the input friction coefficient was determined from the principle of conservation of energy where the energy lost by the pendulum during the swing is equal to the work done in overcoming the friction between the slider and the surface (Giles et al., 1964) i.e.

$$W(H-h) = \mu PD \quad (1)$$

where

- $W$  = effective weight of the swinging arm,
- $H$  = initial height of the center of gravity in the release position,
- $h$  = height of the center of gravity at the highest point of the swing after the slider has passed over the test surface (as indicated by the pointer),
- $\mu$  = effective coefficient of friction between slider and surface,
- $P$  = average normal load between slider and surface, and
- $D$  = sliding distance

The effective weight of the swinging arm ( $W$ ) is 1.486 kg and the average normal force ( $P$ ) is approximately 22 N. The sliding distance ( $D$ ) was selected as 127 mm for the case of flat test specimens. Hence, the corresponding  $\mu$  can be determined for the test specimen based on pendulum measurements.

## 4. FINITE ELEMENT ANALYSIS

### 4.1 Model Verification

The finite element model was first verified against the BPN obtained from the laboratory tests as described in the Section 2. The pendulum measurements from simulation were determined based on kinetic energy loss during the sliding process which corresponds to the difference between the initial kinetic energy and the final kinetic energy of the pendulum at the start and

end of the sliding path respectively. The corresponding pendulum measurement can then be computed using the principle of conservation of energy. Prior to the analysis, the input friction parameter,  $\mu$ , was first determined using Equation (1) based on pendulum measurements obtained from a plain surface test specimen fabricated using Portland cement mortar with the same mixture content as described in Section 2.1. The verification was conducted for dry test condition and the computed  $\mu$  was 0.80. The same value was then used for the various texture patterns for subsequent analyses.

The simulated BPN were compared against the experimental BPN as shown in Table 2. They showed reasonably good agreement with experimental measurements and therefore, verified the validity of the finite element model.

Table 2. Comparison of laboratory and simulated British pendulum measurements

Set- Gap width	Laboratory BPN	Simulated BPN	% Difference
Plain	75.0	75.5	0.65%
A-5mm	82.7	83.0	0.33%
A-10mm	77.0	81.6	5.97%
A-15mm	76.7	79.7	3.92%
A-20mm	74.9	78.4	4.62%
A-25mm	75.3	78.6	4.35%
B-5mm	82.1	81.7	-0.56%
B-10mm	78.9	79.4	0.62%
B-15mm	77.1	79.7	3.33%
C-5mm	91.6	88.9	-2.90%
C-10mm	86.3	94.2	9.10%
C- 15mm	83.8	84.4	0.72%

#### 4.2 Analysis of Test Results

The kinetic energy of the finite element model was obtained from simulation and plotted as shown in Figure 4. The results showed that, in contrast to Set A and B specimens, the kinetic energy of Set C specimens exhibited significant reduction at several instances. Simulation results also revealed that the rubber slider bounced at several instances when it impacted the edges of the rectangular strips of Set C specimens as shown in Figure 5. The phenomenon was verified based on snapshots taken using a high-speed digital camera as shown in Figure 6.

Based on these results, it is likely that the significant increase in BPN as revealed earlier in Section 2 is largely attributed to the edge impact effects between the pendulum slider and the rectangular strips. The slider exhibited significant energy loss when it impacted the edges of the strips. The impact also resulted in the slider bouncing along the surface which would lead to a reduction in the contact area between the slider and the test surface, and thus would give rise to misleading results. On the other hand, there was absence of edge effect associated with Set A and B specimens as shown in Figure 4. The test surfaces of these specimens are closely-packed without surface discontinuities unlike the case of Set C specimens. Hence, it is

likely that the edge effect is a result of surface discontinuities.

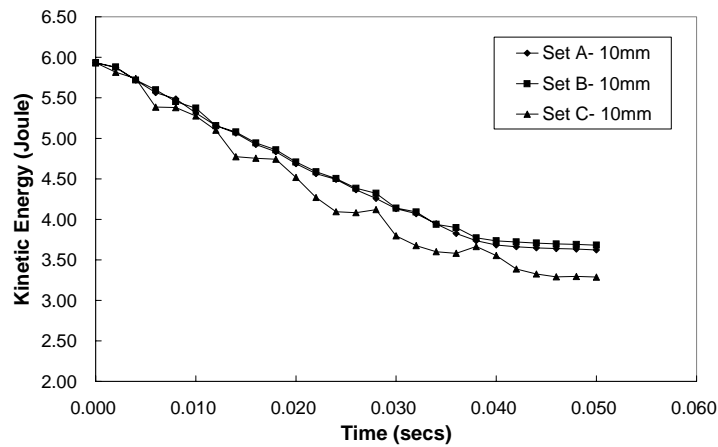


Figure 4. Kinetic energy plots for Set A, B and C specimens for the case of 10 mm aggregate gap width respectively

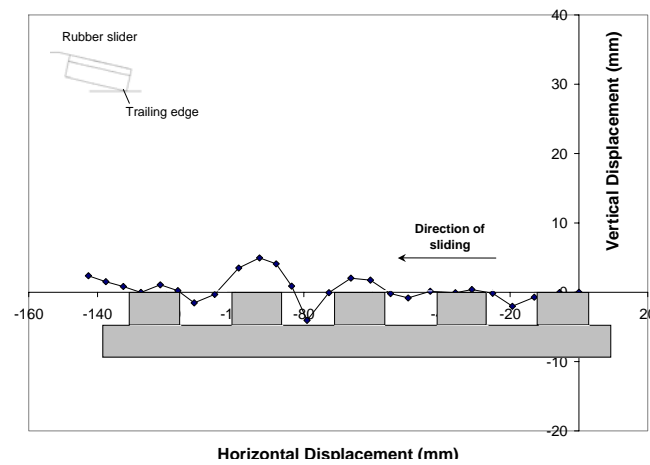


Figure 5. Vertical displacement of trailing edge of rubber slider on Set C- 15 mm gap width

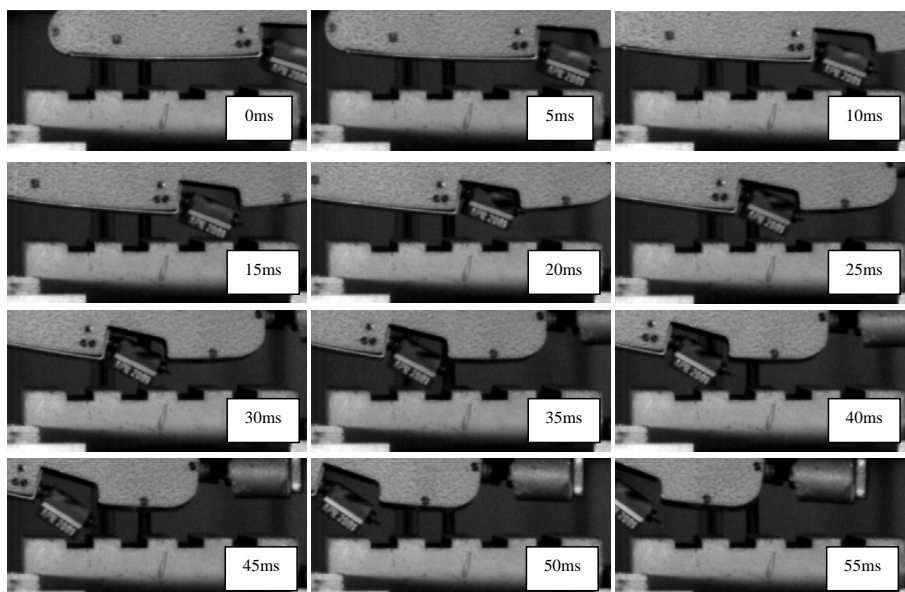
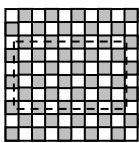
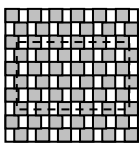
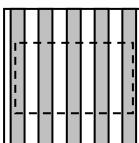
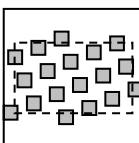
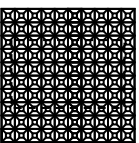
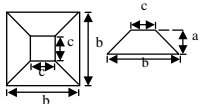


Figure 6. Snapshots of rubber slider on Set C- 15 mm gap width using a highspeed digital camera



To verify the occurrence of edge impacts, several texture patterns were examined using the finite element model in addition to those described in Section 2. The various specimens are presented in Table 3. In this case, sparsely-spaced aggregate patterns (Set D) were introduced to represent coarse-textured surfaces such porous pavement. Hexagonal-shaped aggregates (Set E) were also included in the analysis as they resembled coarse aggregates. In addition, the increase in gap width for Set B specimens was increased from 15 mm to 25 mm.

Table 3. Description of texture patterns for finite element simulation

Set	A	B	C	D	E
Plan View					
Details	Square aggregates with variable size and spacing from 5mm to 25mm	15mm square aggregates with variable gap width from 5mm to 25mm in direction of sliding	15mm wide rectangular strips with variable groove width from 5mm to 15mm in direction of swing	15mm square aggregates with variable staggered gap width from 5mm to 15mm	 Hexagonal aggregates with c/c 15mm and variable top surface area. a= 5mm, b= 15mm, c= 5-10mm

Note: 1) Arrow denotes sliding direction. 2) Broken-line rectangle indicates sliding path. 3) c/c denotes center-to-center spacing.

The simulated BPN results are presented in Figure 7. It can be shown that for closely packed surfaces such as Set A specimens, the BPN showed a decreasing trend with increasing gap width as highlighted in Section 2. However, for Set B specimens, although the BPN decreases initially as gap width increases, the values increased significantly at gap widths more than 15 mm. In this case, the test surface exhibited discontinuities and thus gave rise to the edge impact effects as explained earlier. The effect of edge impacts associated with surface discontinuities was confirmed based on results obtained on Set C, D and E specimens which showed significant increase in BPN as compared to a plain surface. The increase in BPN of these textured surfaces over those of plain surfaces were significantly larger than those of Set A and B specimens especially at gap widths no more than 10 mm, which would lead to over-estimation. On the other hand, the edge impact effects also caused the contact area between the slider and test surface to decrease because of the bouncing of the slider which could explained the erratic changes in BPN as the gap width increases.

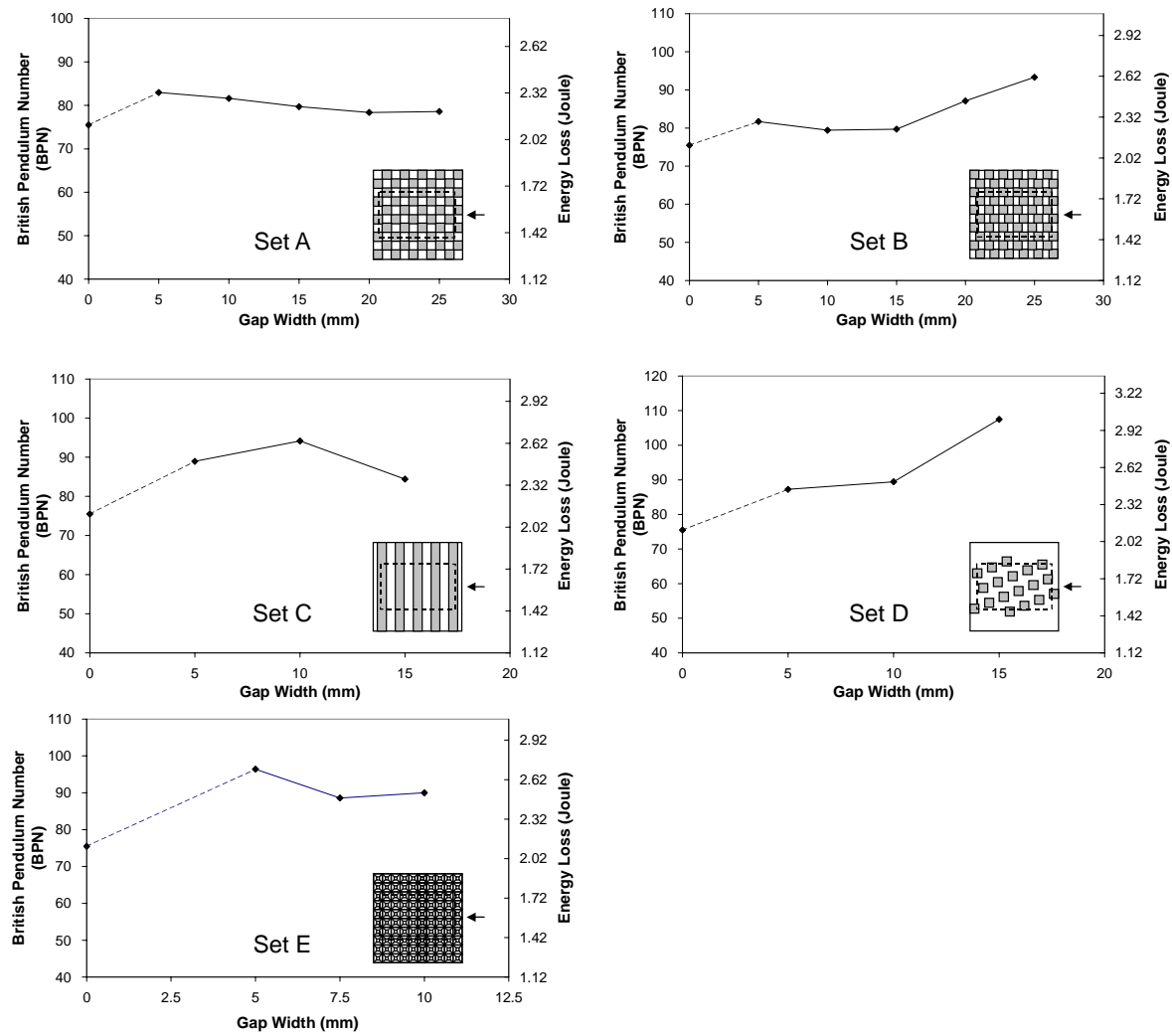


Figure 7. British pendulum measurements obtained from finite element simulation

## 5. CONCLUSIONS

This study demonstrated the effects of macrotexture on the British pendulum measurements. On closely-packed textured surfaces, the measurements were dependent on the surface contact area of the aggregates and aggregate gap width. However, for sparsely-packed textured surfaces or coarse-textured surfaces, the measurements showed significant variations which are attributed to edge impacts between the pendulum slider and coarse-textured surface features. The edge impact effects were associated mainly with textured surfaces which exhibited discontinuities. Simulation results showed that the sliding contact between the pavement surface and the rubber slider of the test device was not maintained as the latter bounced when it impacted on the edges of the textural features. The results demonstrated that the edge impacts between coarse-textured surface features and the pendulum slider would give rise to unreliable test measurements, and care must be exercised in interpretation of the test results.

## REFERENCES

1. American Society for Testing and Materials. (2000) ASTM Standard E 303-93 (Reapproved 1998). Standard Test Method for Measuring Surface Frictional Properties Using the British Pendulum Tester. 2000 Annual Book of ASTM Standards, Vol. 04.03, Philadelphia.
2. Arruda, E. M. and Boyce, M. C. (1993) A Three-Dimensional Constitutive Model for Large Stretch Behavior of Rubber Elastic Materials. **Journal of the Mechanics and Physics of Solids**, Vol. 41, No. 2, pp. 389-412.
3. Forde, M. C., Birse, R. M. and Fraser, D. M. (1976) An Assessment of British Pendulum Based Methods of Skid Resistance Evaluation Using Schonfield's Photo-Interpretation Method. **Proc. 8<sup>th</sup> ARRB Conf.**, 8(4), Session 17, pp. 21-40.
4. Fwa, T. F., Choo, Y. S. and Liu, Y. R. (2003) Effect of Aggregate Spacing on Skid Resistance of Asphalt Pavement. **ASCE Journal of Transportation Engineering**, Vol. 129, No. 4, pp. 420-426.
5. Giles, C. G., Sabey, B. E. and Cardew, K. H. F. (1964) Development and Performance of the Portable Skid Resistance Tester. Road Research Laboratory, Department of Scientific and Industrial Research, **Road Research Technical Paper 66**, HMSO, London.
6. Hibbitt, Karlsson & Sorensen Inc. (2002) **ABAQUS/Explicit** Version 6.3. Pawtucket, Rhode Island, USA.
7. Higdon, A. and Ohlsen, E. H. (1971) **Mechanics of Materials**, 2nd ed., Wiley, New York, USA.
8. Huang, Y. H. (1993) **Pavement Analysis and Design**. Prentice Hall, Inc, pp. 364-367.
9. Lee, Y. P. K., Liu, Y. R., Liu, Y., Fwa, T. F. and Choo, Y. S. (2004) Skid Resistance Prediction by Computer Simulation. 8<sup>th</sup> International Conference on Applications of Advanced Technologies in Transportation Engineering, **Proceedings of the 8<sup>th</sup> AATT Conference**, Beijing, China, 26-28, May, 2004, pp. 465-469.
10. Liu, Y. R., Fwa, T. F. and Choo, Y. S. (2003) Finite Element Modeling of Skid Resistance Test. **ASCE Journal of Transportation Engineering**, Vol. 129, No. 3, pp. 316-321.
11. Liu, Y. R., Fwa, T. F. and Choo, Y. S. (2004) Effect of Surface Macrotecture on Skid Resistance Measurements by the British Pendulum Test. **Journal of Testing and Evaluation**, Vol. 32 (4), pp. 304-309.
12. Moore, D. F. (1972) **The Friction and Lubrication of Elastomers**. Pergammon Press, New York.
13. Purushothaman, N., Heaton, B. S. and Moore, I. D. (1988) Experimental Verification of a Finite Element Contact Analysis. **Journal of Testing and Evaluation**, Vol. 16, No. 6, pp. 497-507.
14. Salt, G. F. (1977) Research on Skid Resistance at the Transport and Research Laboratory (1927-1977), **Transportation Research Record 622**, Transportation Research Board, pp. 26-38.